Single-image superresolution of self-similar textures

Ido Zachevsky

under the supervision of

Prof. Yehoshua Y. Zeevi

May 22, 2013

Introduction

Super-resolution (SR) problem formulation:

$$Y(\eta_1, \eta_2) = \mathcal{D}\left((B * X)(\eta_1, \eta_2)\right) + N(\eta_1, \eta_2)$$

Degradation caused due to both decimation and blur

- Decimation, $\mathcal{D}$, causes aliasing in finitely supported (typically small) PSFs.
- Blur kernel, $B(\eta_1, \eta_2)$: Gaussian, averaging, ...
- Noise, $N(\eta_1, \eta_2)$: iid Gaussian noise, typically with low variance


Original image


Blurred image


BM3D Reconstructed


Blurred+subsampled


BM3D Reconstructed

BM3D is a sparsity-based deblurring algorithm [Danielyan et al., 2012].

Introduction

Super-resolution (SR) problem formulation:

$$Y(\eta_1, \eta_2) = \mathcal{D}\left((B * X)(\eta_1, \eta_2)\right) + N(\eta_1, \eta_2)$$

Degradation caused due to both decimation and blur

- Decimation, $\mathcal{D}$, causes aliasing in finitely supported (typically small) PSFs.
- Blur kernel, $B(\eta_1, \eta_2)$: Gaussian, averaging, ...
- Noise, $N(\eta_1, \eta_2)$: iid Gaussian noise, typically with low variance

Original image

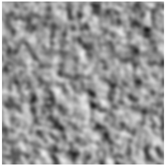

Blurred image

BM3D Reconstructed

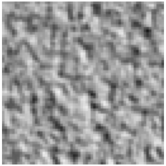

Blurred+subsampled

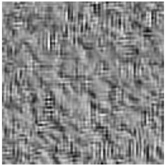

BM3D Reconstructed

BM3D is a sparsity-based deblurring algorithm [Danielyan et al., 2012].

Super-resolution

The super-resolution problem

- Multi-frame super-resolution: Given $\{Y_i(\eta_1, \eta_2)\}_{i=1}^{N}$ [Irani and Peleg, 1990, Elad and Feuer, 1997, Yang and Huang, 2010], ...
- Single-frame super-resolution (upscaling): Given a single measurement, $N = 1$ [Freeman et al., 2002, Glasner et al., 2009, Zeyde et al., 2011]
  - *The focus of this research: Restore a high-resolution image from a single blurred and subsampled observation.*

Texture enhancement

Super-resolution as a specific problem in image enhancement

- Cartoon v. textures - non bounded-variation (BV) space [Gousseau and Morel, 2001]

Methods for texture enhancement

- Differential equations, $I_t = \nabla \cdot (g(|\nabla I|)\nabla I)$ [Gilboa et al., 2002]
  - Complex diffusion with potential [Honigman and Zeevi, 2006]
- Sparseness-based, $X = D\alpha + V$ [Yang et al., 2010]
- Example (learning)-based superresolution [Freeman et al., 2002]
  - Single-image example-based [Glasner et al., 2009]
- Texture synthesis [Efros and Leung, 1999]

Relevance and contribution

Further research is necessary in textured images

Theoretical model

- Analysis of natural images as realizations of random processes
- Interest in the underlying model

Better models may yield better enhancement algorithms

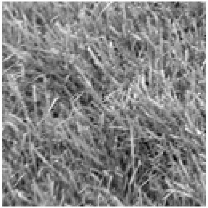

Original image

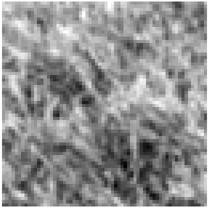

Degraded image

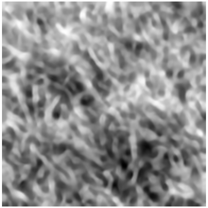

SR [Freeman et al., 2002]

Texture properties

Types of textures [Lin et al., 2004]

- Regular (structured): pattern-based
- Stochastic: based on random processes, $X(\eta_1, \eta_2) = X(\eta_1, \eta_2, \omega)$

Stochastic textures

- Self-similar, $X_c(at) \stackrel{d}{=} |a|^c X_c(t)$
- Long-range dependencies
- Fractal properties [Barnsley, 1988]

For example: fractional Brownian motion.

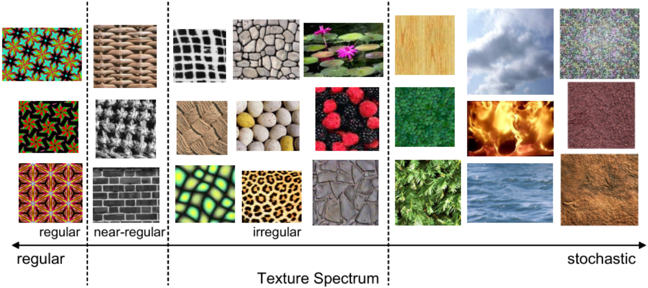

Background

- Image model:

$$Y(\eta_1, \eta_2) = \mathcal{D}\left((B * X)(\eta_1, \eta_2)\right) + N(\eta_1, \eta_2)$$

- Naive solution: $\hat{X}(\eta_1, \eta_2) = (G * Y)(\eta_1, \eta_2)$, where

$$\tilde{G}(\tilde{\eta}_1, \tilde{\eta}_2) = \tilde{B}^{-1}(\tilde{\eta}_1, \tilde{\eta}_2)$$

  Problem: not practical.

- Possible solution: Wiener filtering, Richardson-Lucy deconvolution, L_2-based and TV-based regularization, ...

Regularization

Required for solving ill-posed problems

$$\hat{X}(\eta_1, \eta_2) = \arg\min_X \|Y - \mathcal{D}(B * X)\|_2^2 + \lambda\phi(X)$$

Common regularization functions:

- L_2-based: high gradients are not common, $\phi(x) = \|\nabla X\|_2^2$
- L_1- or TV-based: promotes piecewise-smooth segments

$$\phi(x) = \|\nabla X\|_1$$

- L_p norms, for $p \in (1, 2)$
- L_0 pseudo-norm, promotes sparsity:

$$\phi(\alpha) = \|\alpha\|_0, \; X = D\alpha + V$$

- Reflect an image model (BV space).

Issues

- Restoration results in cartoon images
- Textured details are lost

Outline

1 Introduction

2 Stochastic texture model

3 Generalized stochastic texture model

4 Further research

Fractional Brownian motion

$$E\left[B_H(t)B_H(s)\right] = \frac{\sigma^2}{2}\left(|t|^{2H} + |s|^{2H} - |t-s|^{2H}\right)$$

- Gaussian, self-similar, fractal process [Mandelbrot and Van Ness, 1968]
- The only self-similar Gaussian process (in 1D)
- Brownian motion for $H = 0.5$
- Non-stationary, with stationary increments
- Exhibits negative correlation for $0 < H < 0.5$
- Can be synthesized *efficiently* in 2D by introducing $\phi(\eta_1, \eta_2)$, autocorrelation of the increments.

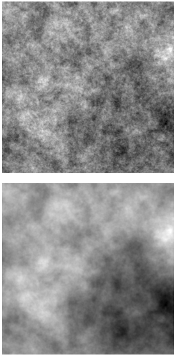

Figure: fBm for $H \in \{0.1, 0.6\}$

Texture model

$$X = X_{LP} + \hat{X}_{HP} + V,$$

where

$$\hat{X}_{HP}(\eta_1, \eta_2) = f\left(\omega, X_{LP}\right)$$

- $X_{LP}(\eta_1, \eta_2)$ is a low-frequency, degraded, image
- $X_{HP}(\eta_1, \eta_2)$ is composed from $\angle X_{LP}$ and an fBm image, $B_H(\eta_1, \eta_2)$
- The high frequencies are an fBm representation of the degraded image

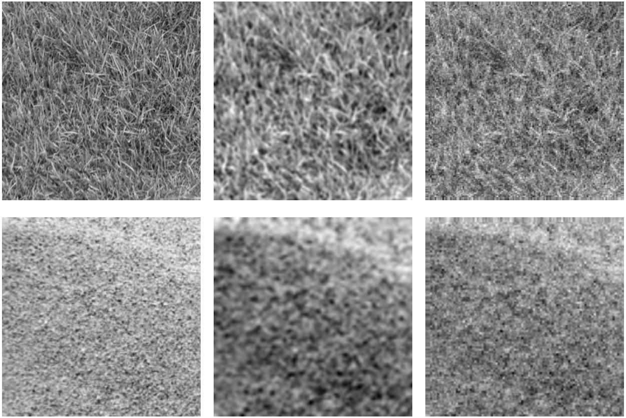

Original image — $X_{LP}(\eta_1, \eta_2)$ — $X(\eta_1, \eta_2)$

Preliminary algorithm

Perform optimization:

$$\begin{aligned}\hat{X} &= \arg\min_{X} \|Y - BX\|^2 \\ s.t. \quad X &= X_{LP} + \hat{X}_{HP} \\ \hat{X}_{HP} &= f(\omega, X_{LP})\end{aligned}$$

Solve by iterating:

1. Apply constraint, $\hat{X} = X_{LP} + \hat{X}_{HP}$
2. Solve proximal point problem,

$$\hat{X}_{k+1} = \arg\min_{X} \|Y - BX\|^2 + \alpha \left\|\hat{X}_k - X\right\|^2$$

- May be considered as a POCS problem

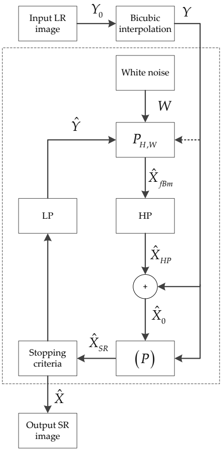

Results

- Performs well on isotropic stochastic textures.
- Recovers missing details according to the model.
- PSNR or MSE-based comparison methods not applicable ($PSNR < 20[dB]$)

Original Degraded Example-based fBm-based

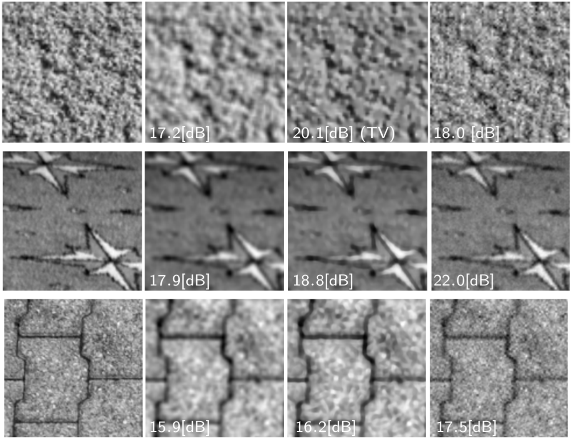

[Zachevsky and Zeevi, 2013]

Outline

1. Introduction
2. Stochastic texture model
3. Generalized stochastic texture model
4. Further research

Disadvantages

The previous model does not perform well on anisotropic, oriented, textures.

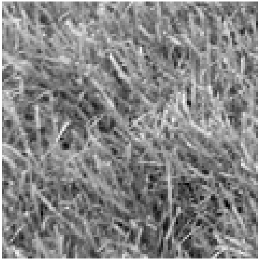

Original

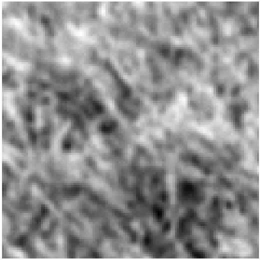

Degraded

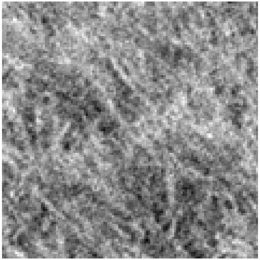

fBm-based

A generalized model is required to handle different orientations in the image.

Tensor diffusion

Basic reaction-diffusion equation for deblurring [Welk et al., 2005]:

$$\begin{aligned}
\hat{X} &= \arg\min_X \|Y - BX\|^2 + \lambda\Psi(\nabla X) \\
X_t &= \underbrace{-B^T * (B * X - Y)}_{\text{Reaction}} + \underbrace{\lambda\nabla \cdot (D(\nabla X)\nabla X)}_{\text{Diffusion}} \\
D &= (\omega_1, \omega_2) \begin{pmatrix} \lambda_1 & 0 \\ 0 & \lambda_2 \end{pmatrix} \begin{pmatrix} \omega_1 \\ \omega_2 \end{pmatrix}
\end{aligned}$$

where

$$\omega_1 \parallel \nabla X, \quad \omega_2 \perp \nabla X$$

- Performs *anisotropic* diffusion, used in various image enhancements tasks
- Applies different diffusion coefficients, according to orientation.
- Can be used for super-resolution.

Tensor diffusion

Incorporation of the model in PDE

- Modified reaction term: $\left(X_{HP} - \hat{X}_{HP}\right)^2$, recovers degraded high frequencies
- Diffusion tensor *modified*: $D\left(\nabla\left(X + \alpha Y_\phi\right)\right)$, preserves texture orientation

New scheme:

$$X_t = 2B^T(BX - Y) - 2H(\hat{X}_{HP} - HX) + \beta\nabla\cdot(\Psi'(|\nabla X + \alpha\nabla Y_\phi|^2)\nabla(X + \alpha Y_\phi))$$

The empirical image, $Y_\phi(\eta_1, \eta_2)$, has the following properties:

- A stochastic image, obtained from the empirical correlations of the degraded image, $Y(\eta_1, \eta_2)$.
- The correlations are suitable for the high-resolution image due to the self-similarity.

Modified diffusion equation

Visualizing the two additions (zoomed-in images)

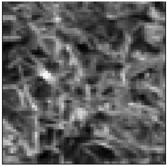

Original image

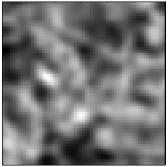

Degraded image

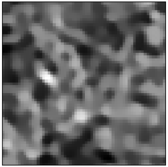

Original PDE

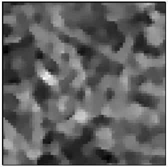

New reaction, $(X_{HP} - \hat{X}_{HP})^2$

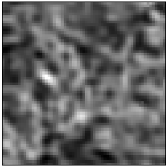

New tensor, $D(\nabla(X + \alpha Y_\phi))$

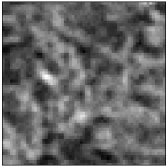

Modified PDE

Comparison with the first algorithm

Recall the previous result

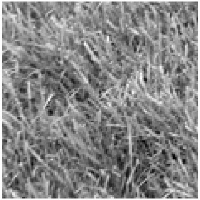

Original

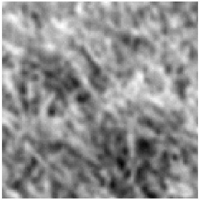

Degraded

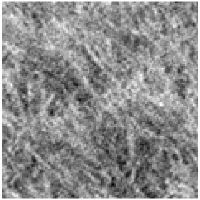

fBm-based

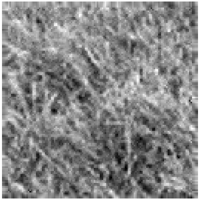

PDE-fBm-based

The current algorithm restores missing details, according to the texture orientation.

Results

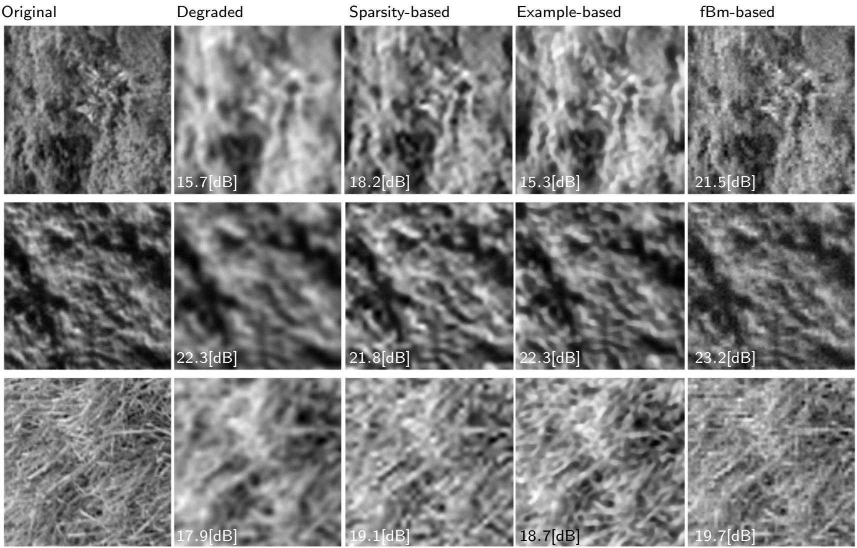

[Zeyde et al., 2011]

Outline

1 Introduction

2 Stochastic texture model

3 Generalized stochastic texture model

4 Further research

Theoretical tasks

- Generalization of the fBm model.
- Geometrical framework
  - Representation in higher spaces and performing color processing [Sochen et al., 1998]

$$C_t = \frac{1}{\sqrt{|g|}} \sum_{\mu,\nu=1}^{2} \partial_\mu \left(\sqrt{|g|} \left(g^{-1} \right)_{\mu,\nu} \partial_\nu C \right)$$

  - Textures as a manifold, embedded in a suitable space, providing an intrinsic metric for comparison [Kimmel et al., 2000].
- Derive a statistical model for textures

Classification and denoising

Classification

- The dominant feature of stochastic textures is self-similarity
- This can be exploited to classify images
- Features: self-similarity index, correlation
- Further features are required
- Segmentation

Image denoising

- Overlap of high-frequency details with that of noise
- The model may prove useful in performing texture denoising

Bibliography I

Aram Danielyan, Vladimir Katkovnik, and Karen Egiazarian. BM3D frames and variational image deblurring. *IEEE Transactions on Image Processing*, 21(4):1715–1728, April 2012. ISSN 1941-0042. doi: 10.1109/TIP.2011.2176954. URL http://www.ncbi.nlm.nih.gov/pubmed/22128008.

Michal Irani and Shmuel Peleg. Super resolution from image sequences. In *Pattern Recognition, 1990. Proceedings., 10th International Conference on*, volume 2, pages 115–120. IEEE Comput. Soc. Press, 1990. ISBN 0-8186-2062-5. doi: 10.1109/ICPR.1990.119340. URL http://ieeexplore.ieee.org/lpdocs/epic03/wrapper.htm?arnumber=119340.

Michael Elad and Arie Feuer. Restoration of a single superresolution image from several blurred, noisy, and undersampled measured images. *Image Processing, IEEE Transactions on*, 6(12):1646–1658, January 1997. ISSN 1057-7149. doi: 10.1109/83.650118. URL http://www.ncbi.nlm.nih.gov/pubmed/18285235.

Jianchao Yang and Thomas Huang. Image super-resolution: Historical overview and future challenges. *Super-resolution imaging*, 2010.

William T Freeman, Thouis R Jones, and Egon C Pasztor. Example-Based Super-Resolution. *Computer Graphics and Applications, IEEE*, 22(2):56–65, 2002.

Daniel Glasner, Shai Bagon, and Michal Irani. Super-resolution from a single image. *2009 IEEE 12th International Conference on Computer Vision*, pages 349–356, September 2009. doi: 10.1109/ICCV.2009.5459271. URL http://ieeexplore.ieee.org/lpdocs/epic03/wrapper.htm?arnumber=5459271.

Roman Zeyde, Michael Elad, and Matan Protter. On Single Image Scale-Up Using Sparse-Representations. In *Curves and Surfaces*, number 1, pages 711–730. 2011.

Yann Gousseau and Jean-Michel Morel. Are Natural Images of Bounded Variation? *SIAM Journal on Mathematical Analysis*, 33(3):634–648, January 2001. ISSN 0036-1410. doi: 10.1137/S0036141000371150. URL http://epubs.siam.org/doi/abs/10.1137/S0036141000371150.

Bibliography II

Guy Gilboa, Nir Sochen, and Yehoshua Y Zeevi. Forward-and-backward diffusion processes for adaptive image enhancement and denoising. *IEEE Transactions on Image Processing*, 11(7):689–703, January 2002. ISSN 1057-7149. doi: 10.1109/TIP.2002.800883. URL http://www.ncbi.nlm.nih.gov/pubmed/18244666.

Ori Honigman and Yehoshua Y. Zeevi. Enhancement of Textured Images Using Complex Diffusion Incorporating Schrodinger's Potential. In *ICASSP*, pages 633–636, 2006.

Jianchao Yang, John Wright, Thomas Huang, and Yi Ma. Image Super-Resolution via Sparse Representation. *Image Processing, IEEE Transactions on*, 19(11):2861–2873, May 2010. ISSN 1941-0042. doi: 10.1109/TIP.2010.2050625. URL http://www.ncbi.nlm.nih.gov/pubmed/20483687.

Alexei A Efros and Thomas K Leung. Texture synthesis by non-parametric sampling. *Proceedings of the 7th IEEE International Conference on Computer Vision*, 2:1033–1038, 1999. doi: 10.1109/ICCV.1999.790383. URL http://ieeexplore.ieee.org/lpdocs/epic03/wrapper.htm?arnumber=790383.

Wen-Chieh Lin, James Hays, Chenyu Wu, Vivek Kwatra, and Yanxi Liu. *A comparison study of four texture synthesis algorithms on regular and near-regular textures*. Number January. Citeseer, 2004. URL http://citeseerx.ist.psu.edu/viewdoc/download?doi=10.1.1.5.6067&rep=rep1&type=pdf.

Michael F Barnsley. *Fractals everywhere*, volume 19. Academic Press Professional, Inc., 1988.

Benoit B Mandelbrot and John W Van Ness. Fractional Brownian motions, fractional noises and applications. *SIAM review*, 10(4):422–437, 1968.

Ido Zachevsky and Yehoshua Y. Zeevi. Single-image superresolution of self-similar textures. In *IEEE International Conference on Image Processing (accepted)*, 2013.

Martin Welk, David Theis, Thomas Brox, and Joachim Weickert. PDE-based deconvolution with forward-backward diffusivities and diffusion tensors. *Scale Space and PDE Methods in Computer Vision*, pages 585–597, 2005. URL http://link.springer.com/chapter/10.1007/11408031_50.

Bibliography III

Nir Sochen, Ron Kimmel, and Ravikanth Malladi. A general framework for low level vision. *IEEE transactions on image processing*, 7(3):310–8, January 1998. ISSN 1057-7149. doi: 10.1109/83.661181. URL http://www.ncbi.nlm.nih.gov/pubmed/18276251.

Ron Kimmel, Nir A Sochen, and Ravi Malladi. On the Geometry of Texture. Technical report, 2000.

Stephan Hoefer, H Hannachi, Madhukar Pandit, and Ramdas Kumaresan. Isotropic Two-Dimensional Fractional Brownian Motion and its Application in Ultrasonic Analysis. In *Engineering in Medicine and Biology Society, 1992 14th Annual International Conference of the IEEE*, pages 1267–1269, 1992. ISBN 0780307852.

Lance M Kaplan and C-CJ Kuo. An improved method for 2-D self-similar image synthesis. *Image Processing, IEEE Transactions on*, 5(5):754–761, January 1996. ISSN 1057-7149. doi: 10.1109/83.495958. URL http://www.ncbi.nlm.nih.gov/pubmed/18285164.

Pietro Perona and Jitendra Malik. Scale-space and edge detection using anisotropic diffusion. *IEEE Transactions on Pattern Analysis and Machine Intelligence*, 12(7):629–639, July 1990. ISSN 01628828. doi: 10.1109/34.56205. URL http://ieeexplore.ieee.org/lpdocs/epic03/wrapper.htm?arnumber=56205.

Joachim Weickert. *Anisotropic Diffusion in Image Processing*. Teubner Stuttgart, 1998.

Béatrice Pesquet-Popescu and Pascal Larzabal. Synthesis of nonstationary fields with stationary increments. *Image Processing and Its Applications*, 1:303–307, 1997.

Helge von Koch. On a Continuous Curve Without Tangent Constructable from Elementary Geometry. *Classics on fractals*, 1904.

Thank you

Backup

Fractional Brownian motion synthesis

1. Naive [Hoefer et al., 1992]: Construct $R_B(t,s)$, the autocorrelation function of the fBm:

$$\begin{aligned} E\left[B_H(t)B_H(s)\right] &= \frac{\sigma^2}{2}\left(|t|^{2H} + |s|^{2H} - |t-s|^{2H}\right) \\ \sigma_B^2 &= \frac{\sigma_B^2}{2}\frac{\cos(\pi H)}{\pi H}\Gamma(1-2H) \end{aligned}$$

   Inefficient due to use of Cholesky decomposition.

2. Via the Fourier domain [Kaplan and Kuo, 1996]:
   - First- and second-order increments are stationary.
   - Their autocorrelations are expressed via a structure function, $\phi(\eta_1, \eta_2)$.
   - Fields with these autocorrelation functions can be efficiently synthesized via the Fourier domain.
   - 2D fBm is obtained by summation of the increments.

Back

Anisotropic diffusion

Non-linear isotropic diffusion [Perona and Malik, 1990]

$$X_t = \nabla \cdot (g(|\nabla X_\sigma|)\nabla X)$$
$$g(s^2) = \frac{1}{1+\left(\frac{s^2}{K^2}\right)}$$

- Adaptive: diffusion coefficient inversely proportional to norm of gradient
- Done isotropically, regardless of orientation

Weickert anisotropic diffusion [Weickert, 1998]:

$$X_t = \nabla \cdot (D(\nabla X)\nabla X)$$
$$D = (\omega_1, \omega_2)\begin{pmatrix}\lambda_1 & 0 \\ 0 & \lambda_2\end{pmatrix}\begin{pmatrix}\omega_1 \\ \omega_2\end{pmatrix}$$

- For edge preserving denoising: λ_1 similar to Perona and Malik, and λ_2=0.1. Enhances edges according to orientation.

Back

Modified diffusion equation

- A nonstationary field with stationary increments can be synthesized using a generating (structure) function, $\phi(\eta_1, \eta_2)$ [Pesquet-Popescu and Larzabal, 1997]:

$$\begin{aligned}\phi(\Delta_1, \Delta_2) &= var\left(F(\eta_1, \eta_2) - F(\eta_1 - \Delta_1, \eta_2 - \Delta_2)\right)\\ \phi_{fBm}(\Delta_1, \Delta_2) &= (\Delta_1^2 + \Delta_2^2)^H \triangleq r^{2H}\end{aligned}$$

- The empirical image, $Y_\phi(\eta_1, \eta_2)$, is obtained by an inverse process using an empirical structure function.

$$\hat{\phi}(\eta_1, \eta_2) = f_1(Y(\eta_1, \eta_2)) \quad \Rightarrow \quad \hat{B}_{\hat{\phi}}(\eta_1, \eta_2) = f_2(\hat{\phi}, \omega)$$

- Due to the self similarity, the correlations are suitable for the superresolution image.

Modified diffusion equation

- The inverse process is performed via solving an ill-posed least squares problem:

$$\underline{\phi} = \arg\min_{\underline{x}} \|D\underline{x} - \underline{r}\|_2$$

- Further methods can be explored to find more suitable empirical structure functions.

Example:

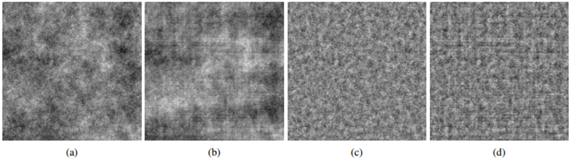

Figure: Original fBm, fBm from $\phi(\eta_1, \eta_2)$ and high-pass versions

Back

Empirical function in algorithm progress

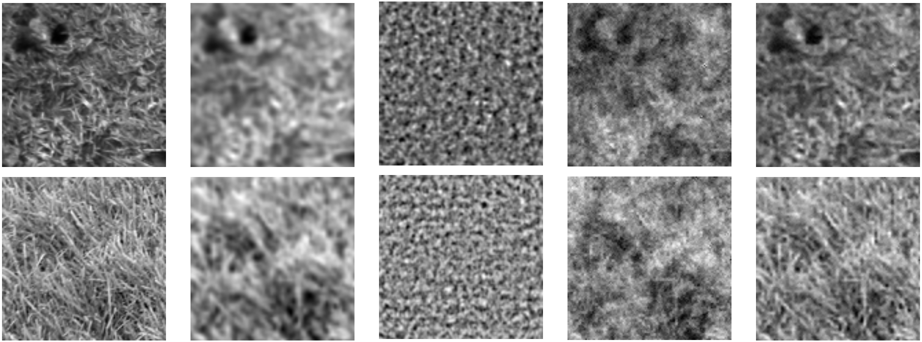

Original image | Degraded image | $Y_\phi(\eta_1, \eta_2)$ | $\hat{X}(\eta_1, \eta_2)$ | Enhanced image

- Further study necessary for empirical image. Back

Further research

Geometric fractals

- Geometric fractals appear in various natural images.
- The structure can be exploited for an image model and SR scheme.

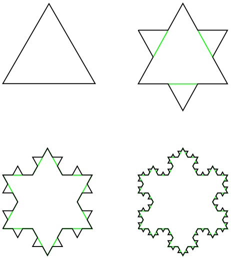

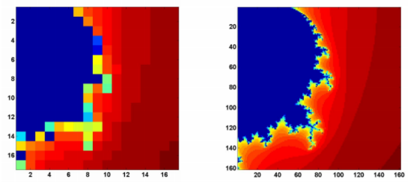

Mandelbrot set [Barnsley, 1988]

Koch snowflake [von Koch, 1904]